Time optimal control for a perturbed Brockett integrator

Jérôme Lohéac, Jean-Francois Scheid

Time optimal control for a perturbed Brockett integrator

Application to time optimal axi-symmetric micro-swimmers

Jérôme Lohéac[1] and Jean-François Scheid[2]

[1]LUNAM Université, IRCCyN UMR CNRS 6597, École des Mines de Nantes, 4 rue Alfred Kastler, 44307 Nantes, France.
[2]IECL - Institut Élie Cartan de Lorraine, UMR 7502, Université de Lorraine, Campus des Aiguillettes, B.P. 70239, 54506 Vandoeuvre-lès-Nancy Cedex, France.

jerome.loheac@irccyn.ec-nantes.fr, jean-francois.scheid@univ-lorraine.fr

Abstract

The aim of this work is to compute time optimal controls for a perturbation of a Brockett integrator with state constraints. Brockett integrator and its perturbations appears in many applications fields. One of them described in details in this note is the swimming of micro-organisms. We present some key results for a *fast* and *robust* numerical method to compute time optimal controls for the perturbation of a Brockett integrator. This numerical method is based on explicit formulae of time optimal controls for the Brockett integrator. The methodology presented in this work is applied to the time optimal control of a micro-swimmer.

Keywords. Time optimal controllability, State constraints, Numerical resolution, Brockett integrator, Micro-swimmers.

AMS classification. 34H05, 49J15, 49K15, 49K20, 93C15.

1 Introduction

In this paper, we consider the system:

$$\dot{h} = \langle V(\alpha), \lambda \rangle \tag{1.1a}$$

$$\dot{\alpha} = \lambda\,, \tag{1.1b}$$

where $(h, \alpha) \in \mathbb{R} \times \mathbb{R}^n$ are the state variables, $\lambda \in \mathbb{R}^n$ is the control variable and $V : \mathbb{R}^n \to \mathbb{R}^n$ is a given map. In (1.1a), $\langle \cdot, \cdot \rangle$ denotes the Euclidean product in $\mathbb{R}^n$. The system (1.1a), (1.1b) is completed with the initial conditions:

$$h(0) = 0 \qquad \text{and} \qquad \alpha(0) = 0\,. \tag{1.1c}$$

The first aim of this work is the following. Given $T > 0$, $h^f \in \mathbb{R}^*$ and $c > 0$, find a control $\lambda : [0, T] \to \mathbb{R}^n$ such that the final target h^f is reached at time T:

$$h(T) = h^f \qquad \text{and} \qquad \alpha(T) = 0\,, \tag{1.2}$$

together with the state constraint:

$$|\alpha(t)| \leqslant c \qquad (t \in [0, T])\,, \tag{1.3}$$

where $|\cdot|$ denotes the Euclidean norm in $\mathbb{R}^n$.

Providing that $V \in C^\infty(\mathbb{R}^n, \mathbb{R}^n)$ and the Jacobian matrix $\nabla V(0) \in M_n(\mathbb{R})$ is not symmetric, we prove that this control problem can be solved. More precisely, there exists a minimal time $T^\star = T^\star(h^f, c) > 0$ such that the control problem (1.1)-(1.3) admits a solution $\lambda \in BV([0,T], \mathbb{R}^n)$ together with the control constraint:

$$|\lambda(t)| \leqslant 1 \qquad (\text{for a.e. } t \in [0,T])\,. \tag{1.4}$$

The second aim of this work which actually constitutes the main issue of this note, is to present an efficient numerical method for the computation of time optimal controls for the system (1.1)-(1.4). The method relies on explicit optimal solutions given in [22] for the time optimal control problem (1.1)-(1.4) with $V(\alpha) = M\alpha$ where $M \in M_n(\mathbb{R})$ is a non-symmetric matrix. The numerical method is also based on a full direct discretization as depicted in [30, § 9.II.1]. Let us mention that (1.1) with $V(\alpha) = M\alpha$ is a natural extension of the Brockett integrator:

$$\begin{aligned} \dot{h} &= \alpha_2\lambda_1 - \alpha_1\lambda_2\,, \\ \dot{\alpha}_1 &= \lambda_1\,, \\ \dot{\alpha}_2 &= \lambda_2\,. \end{aligned}$$

Roughly speaking, up to some adaptations, our numerical method is a full direct discretization method (see [30, § 9.II.1]) initialized with the analytic solution obtained in [22] for $M = \nabla V(0)$. Numerical examples will show that this initialisation procedure provides better results than arbitrary initial guesses. It improves the robustness and reduces the computational time.

This strategy is applied to the time optimal control of micro-swimmers. We will see that the efficiency of the micro-swimmer we consider is low and the minimal time is high. Our strategy also provides a preliminary estimate of the minimal control time and hence we also get an estimate of the time discretization step required for suitable results. In this note, we only focus on numerical results. No theoretical proof of robustness nor algorithmic complexity are given. We emphasize that even if direct discretization methods are robust for control problems, knowing an approximation of the optimal solution is even better.

Moreover, in this note, for the sake of clarity, we only present the dimension case $n = 2$, but a similar methodology can be obtained for any $n \geqslant 2$.

This note is organized as follows. We first give controllability and time optimal controllability results for the control problem (1.1)-(1.4) in section 2. Analytic results obtained in [22] are recall in section 3. In section 4, we present the numerical strategy and its application to time optimal micro-swimmers is studied in section 5.

2 Controllability and time optimal controllability

Using Chow Theorem, the following controllability result holds.

Proposition 2.1. *Let $c > 0$ and $V \in C^\infty(\mathbb{R}^2, \mathbb{R}^2)$ be given and assume that the Jacobian matrix $\nabla V(0)$ is not symmetric i.e. :*

$$\nabla V(0) \neq (\nabla V(0))^\top\,.$$

Then, for every $h^f \in \mathbb{R}^*$ and every $T > 0$, there exists $\lambda \in C^0([0,T], \mathbb{R}^2)$ with $|\lambda(t)| \leqslant 1$ for all $t \in [0,T]$ such that the solution of (1.1) satisfies the final condition (1.2) together with the state constraint (1.3).

Proof. Let us write $f_1(h,\alpha) = \big(V_1(\alpha),\, 1,\, 0\big)^\top$ and $f_2(h,\alpha) = \big(V_2(\alpha),\, 0,\, 1\big)^\top$ for $V(\alpha) = (V_1(\alpha),\, V_2(\alpha))^\top$. The system (1.1) becomes:

$$\frac{\mathrm{d}}{\mathrm{d}t}\begin{pmatrix} h \\ \alpha \end{pmatrix} = \lambda_1 f_1(h,\alpha) + \lambda_2 f_2(h,\alpha)\,.$$

The Lie bracket of f_1 and f_2 at the point 0 is given by:

$$[f_1, f_2]_0 = \begin{pmatrix} \partial_{\alpha_1} V_2(0) - \partial_{\alpha_2} V_1(0) \\ 0 \\ 0 \end{pmatrix},$$

which does not vanish if $\nabla V(0)$ is not a symmetric matrix. Thus, under this assumption, the Lie algebra generated by $\{f_1, f_2\}$ and evaluated at the point 0 is of dimension 3. In addition, this Lie algebra is independent of h and the fist order Lie bracket is continuous with respect to α. Therefore, there exists $\varepsilon > 0$ such that for every $(h, \alpha) \in \mathbb{R} \times B_0(\varepsilon)$, the Lie algebra generated by $\{f_1, f_2\}$ evaluated at the point (h, α) is of dimension 3.
The result follows from Chow's Theorem (see for instance [30, chap. 5, Proposition 5.14], [1] or [17]). □

This result combined with the Filippov Theorem (see for instance [1, 10, 16]) leads to the following optimal control result:

Proposition 2.2. *Let $c > 0$ and $V \in C^\infty(\mathbb{R}^2, \mathbb{R}^2)$ such that $\nabla V(0) \neq (\nabla V(0))^\top$. Then, the set of times $T > 0$ such that there exists $\lambda \in BV(0,T)^2$ with $|\lambda(t)| \leqslant 1$ for almost every time $t \in [0,T]$ and such that the solution (h, α) of (1.1) satisfies the final condition (1.2) together with the state constraint (1.3) on α, admits a minimum value $T^\star = T^\star(h^f, c) > 0$.*

Remark 2.3.
1. *The constraint $|\lambda(t)| \leqslant 1$ on the control variable λ is necessary to make the time minimal control problem relevant. Without this constraint, one can build a sequence of time $(T_n)_n \in (\mathbb{R}_+^*)^{\mathbb{N}}$ and associated controls $\lambda_n \in BV(0,T_n)^2$ solving the control problem such that $T_n \to 0$. Thus, the corresponding time optimal control does not make sense.*
2. *As in [22, Proposition 3.3], it can be proved that if λ is a time optimal control, then $|\lambda(t)| = 1$ for almost every $t \in [0, T^\star]$. Consequently, the control variable can be written as $\lambda(t) = R(\Theta(t))$ for almost every t, with $\Theta(t) \in \mathbb{R}$ and*

$$R(\theta) = \begin{pmatrix} \cos\theta & -\sin\theta \\ \sin\theta & \cos\theta \end{pmatrix} \qquad (\theta \in \mathbb{R}), \tag{2.5}$$

denotes the rotation matrix of angle θ.

3 An approximate linearized time optimal control problem

For a small parameter $c > 0$, we have $V(\alpha) = V(0) + \nabla V(0)\alpha + o(c)$ for every $\alpha \in B_0(c)$. Instead of considering the time optimal controllability of the system (1.1), we first consider the approximated linear system:

$$\dot{h} = \langle V(0) + \nabla V(0)\alpha,\ \lambda \rangle\ , \tag{3.6a}$$
$$\dot{\alpha} = \lambda\,, \tag{3.6b}$$

with the initial condition (1.1c).
We assume that the Jacobian matrix of V at $\alpha = 0$ is not symmetric. Thus, Proposition 2.2 ensures the existence of a minimal time $T^\star$ such that the solution (h, α, λ) of the control problem (3.6) with initial condition (1.1c) satisfies (1.2) together with (1.3) and (1.4). In addition, according to [22, Proposition 7], this optimal time $T^\star$ and time optimal controls can be explicitly computed.

Proposition 3.1. *Let $h^f \neq 0$, $c > 0$ and $V \in C^\infty(\mathbb{R}^2, \mathbb{R}^2)$. Let $\gamma \in \mathbb{R}$ such that $\gamma J = \frac{1}{2}\left(\nabla V(0) - (\nabla V(0))^\top\right)$ with $J = \begin{pmatrix} 0 & -1 \\ 1 & 0 \end{pmatrix}$. Assume $\gamma \neq 0$ and define:*

$$d^\star = \sqrt{\frac{2|h^f|}{\pi|\gamma|}} \qquad \text{and} \qquad \tau = \frac{\pi c}{2}\,.$$

Then, the minimal time $T^\star$ of the control problem (3.6), (1.1c), (1.2), (1.3) *and* (1.4) *is given by:*

$$T^\star = \begin{cases} \pi d^\star & \text{if } c \geqslant d^\star\,, \\ \dfrac{\pi (d^\star)^2}{2c} + \tau & \text{otherwise.} \end{cases}$$

Moreover, the time optimal control $\lambda^\star$ is continuous and given by:

$$\lambda^\star(t) = R\left(\Theta(t) + \Theta_0\right) \begin{pmatrix} 1 \\ 0 \end{pmatrix} \qquad (t \in [0, T^\star])\,;$$

where, for every $\theta \in \mathbb{R}$, $R(\theta)$ is the rotation matrix of angle θ defined by (2.5), *Θ_0 is any real constant and $\Theta(t)$ is given by:*

- *If $c \geqslant d^\star$,*

$$\Theta(t) = \operatorname{sign}(\gamma h^f) 2\pi \frac{t}{T^\star} \qquad (t \in [0, T^\star])\,;$$

- *if $c < d^\star$,*

$$\Theta(t) = \begin{cases} \operatorname{sign}(\gamma h^f)\pi \dfrac{t}{\tau} & \text{if } t \in [0, \tau)\,, \\ \operatorname{sign}(\gamma h^f)\pi \dfrac{t+\tau}{2\tau} & \text{if } t \in [\tau, T^\star - \tau]\,, \\ \operatorname{sign}(\gamma h^f)\pi \dfrac{t+\tau-\frac{T^*}{2}}{\tau} & \text{if } t \in (T^\star - \tau, T^\star]\,. \end{cases}$$

Proof. Since $\alpha(0) = \alpha(T)$, it can be easily proved that λ is a control on $[0, T]$ for the system (3.6), (1.1c)-(1.4) if and only if λ is a control on $[0, T]$ for the following system:

$$\dot{h} = \left\langle \tfrac{1}{2}\big(\nabla V(0) - (\nabla V(0))^\top\big)\alpha,\, \lambda \right\rangle\,, \tag{3.7a}$$

$$\dot{\alpha} = \lambda\,, \tag{3.7b}$$

together with (3.6), (1.1c)-(1.4). The result follows from [22, Proposition 7]. □

Remark 3.2. *Let us explain the formulae of the optimal solution given in Proposition 3.1. The optimal deformation $\alpha^\star(t) = \int_0^t \lambda^\star(s)\,\mathrm{d}s$ possesses the following characteristics (see Figure 1):*

- *If $c \geqslant d^\star$, the optimal trajectory $t \mapsto \alpha^\star(t)$ is a circle of diameter $d^\star$, starting from* 0*;*
- *if $c < d^\star$, the optimal trajectory $t \mapsto \alpha^\star(t)$ is composed of three arcs of circle. The first arc of circle is an half-circle of diameter c, starting from* 0 *. The second one lies on the circle of diameter $2c$, centred at the origin* 0*. Finally, the third arc of circle is a half-circle of diameter c, reaching the origin* 0 *at the final time $t = T^\star$.*

4 Numerical computation of a time optimal trajectory

In this section, we will explain our numerical approach for computing optimal trajectories, which is mainly inspired from [30, § 9.II.1].

4.1 Finite dimensional minimisation problem

Let us rewrite our time optimal control problem as a general optimisation problem. First of all, we consider a time control $\bar{T}$ (i.e. a time that solves the control problem (1.1)-(1.4)), so that the

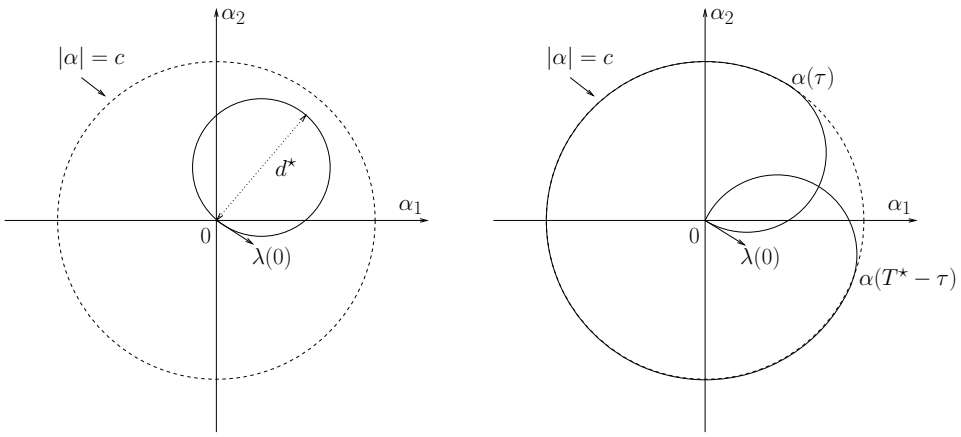

(a) Case $c \geqslant d^\star$. (b) Case $c < d^\star$.

Figure 1: Typical time optimal trajectories of $\alpha = (\alpha_1\ \alpha_2)^\top$.

minimal time $T^\star$ is lower than $\bar{T}$ and we define the cost function $\mathcal{J}_0 : (T, \lambda) \in [0, \bar{T}] \times BV(0, \bar{T})^2 \mapsto T \in \mathbb{R}$. The optimisation problem reads as follows:

$$\begin{array}{ll} \min & T = \mathcal{J}_0(T, \lambda) \\ & (T, \lambda) \in [0, \bar{T}] \times BV(0, \bar{T})^2\,, \\ & |\lambda(t)| \leqslant 1 \qquad (\text{for a.e. } t \in [0, T])\,, \\ & |\alpha(t)| \leqslant c \qquad (t \in [0, T])\,, \\ & \alpha(0) = \alpha(T) = 0\,, \\ & h(0) = 0\,, \quad \text{and} \quad h(T) = h^f\,, \\ & \text{where } \alpha \text{ and } h \text{ are solutions of } \left\{ \begin{array}{l} \dot{h} = \langle V(\alpha), \lambda \rangle\,, \\ \dot{\alpha} = \lambda\,. \end{array} \right. \end{array}$$

According to item 2 of Remark 2.3, any optimal solution λ satisfies $|\lambda(t)| = 1$ for almost every t and hence it can be expressed as $\lambda(t) = R(\Theta(t))e_1$ for almost every t, with $e_1 = (1, 0)^\top$. The state variable α is also given by $\alpha(t) = \int_0^t R(\Theta(s))e_1\,\mathrm{d}s$. Then, we introduce the new cost function $\mathcal{J}_1 : (T, \Theta) \in [0, \bar{T}] \times BV(0, \bar{T}) \mapsto T \in \mathbb{R}$ and the above optimisation problem can be simplified to:

$$\begin{array}{ll} \min & T = \mathcal{J}_1(T, \Theta)\,, \\ & (T, \Theta) \in [0, \bar{T}] \times BV(0, \bar{T})\,, \\ & \left| \int_0^t R(\Theta(s))e_1\,\mathrm{d}s \right| \leqslant c \qquad (t \in [0, T])\,, \\ & \int_0^T R(\Theta(t))e_1\,\mathrm{d}t = 0\,, \\ & \int_0^T \left\langle V\left(\int_0^t R(\Theta(s))e_1\,\mathrm{d}s \right),\, R(\Theta(t))e_1 \right\rangle \mathrm{d}t = h^f\,. \end{array} \tag{4.8}$$

In order to numerically tackle this problem, we set $n \in \mathbb{N}^*$ an integer and $t_0 < \cdots < t_n$ $n+1$ time discretization points. For every $i \in \{0, \cdots, n\}$, we consider $\Theta_i \in \mathbb{R}$ an approximation of $\Theta(t_i)$. Let us also define a quadrature formula $\mathcal{I}(t_0, \cdots, t_k; f_0, \cdots, f_k)$ approximating $\int_{t_0}^{t_k} f(s)\,\mathrm{d}s$ with $f_i = f(t_i)$.
Thus, defining the cost function $J_n : (T, \Theta_0, \cdots, \Theta_n) \in \mathbb{R}_+ \times \mathbb{R}^{n+1} \mapsto T \in \mathbb{R}$, the discretized version

of (4.8) is:

$$\begin{array}{ll}\min & T = J_n(T,\Theta_0,\cdots,\Theta_n)\,,\\ & \left(T,\Theta_0,\cdots,\Theta_n\right)\in\mathbb{R}_+\times\mathbb{R}^{n+1}\,,\\ & |\alpha_k|\leqslant c \qquad (k\in\{1,\cdots,n-1\})\,,\\ & \mathcal{I}\left(0,\frac{T}{n},\cdots,\frac{(n-1)T}{n},T;R(\Theta_0)e_1,\cdots,R(\Theta_n)e_1\right)=0\,,\\ & \mathcal{I}\left(0,\frac{T}{n},\cdots,\frac{(n-1)T}{n},T;\langle V(\alpha_0),R(\Theta_0)e_1\rangle,\cdots,\langle V(\alpha_n),R(\Theta_n)e_1\rangle\right)=h^f\,,\\ & \quad\text{with } \alpha_k=\mathcal{I}\left(0,\frac{T}{n},\cdots,\frac{kT}{n};R(\Theta_0)e_1,\cdots,R(\Theta_k)e_1\right),\ \text{for } k\in\{0,\cdots,n\}\,.\end{array}\tag{4.9}$$

This nonlinear minimisation problem can be solved for instance with an interior-point method, SQP (sequential quadratic programming) or an active-set algorithm (see e.g. [7, 9, 13]) as implemented is the Optimization toolbox of MATLAB through the `fmincon` function. We will see on practical examples that even if the interior point algorithm is robust with respect to the initialisation, the better the initialisation guess is, the better the result is.

A natural initialisation procedure is to use the time optimal control obtained analytically for the linearized problem with $\nabla V(0)\alpha$ in place of $V(\alpha)$.

4.2 Numerical example

Let us consider:

$$V(\alpha)=\begin{pmatrix}-\alpha_2+\alpha_2^2+10\alpha_2^3\\ \alpha_1+\alpha_1^2\end{pmatrix}.\tag{4.10}$$

For the computation of the integrals in the minimisation problem, we use the trapeze method, i.e., for $f\in C([\tau_0,\tau_1],\mathbb{R})$, we approximate $\int_{\tau_0}^{\tau_1} f(t)\,\mathrm{d}t$ by:

$$\mathcal{I}(t_0,\cdots,t_n;f_0,\cdots,f_n)=\sum_{k=1}^{n}\frac{t_k-t_{k-1}}{2}(f_{k-1}+f_k)\,,\tag{4.11}$$

with $t_k=\tau_0+\frac{k(\tau_1-\tau_0)}{n}$ and $f_k=f(t_k)$.

In order to numerically solve the optimisation problem (4.9) with (4.10), we use the `fmincon` function of the Optimization toolbox of MATLAB with a SQP (sequential quadratic programing) algorithm.A first observation is that if we choose the initial value $(T,\Theta_0,\cdots,\Theta_n)=(1,0,\cdots,0)$, the algorithm is not converging. On the other hand, when initializing with the optimal solution of the approximate linearized problem (3.6),(1.1c),(1.2)-(1.4) (see Section 3), we obtain a reasonable solution to the nonlinear optimisation problem (4.9) (see Figure 2).

The SQP algorithm with the trivial initialisation point $(T,\Theta_0,\cdots,\Theta_n)=(1,0,\cdots,0)$ fails to converge because the discrete state trajectory $\alpha_0,\cdots,\alpha_n$ associated to this control does not fill the state constraint $|\alpha_k|\leqslant c$ in (4.9). Indeed, for the initial value $(T,\Theta_0,\cdots,\Theta_n)=(1,0,\cdots,0)$, due to (4.11) we have $\alpha_k=t_ke_1$ for all $k\in\{1,\cdots,n\}$ and in particular we get $|\alpha_n|=|Te_1|=T=1$. A way to avoid this is to use the initialisation point:

$$(T,\Theta_0,\cdots,\Theta_n)=(1,0,\pi,\cdots,n\pi)\,,\tag{4.12}$$

so that the discrete state variables associated to this control are given by $\alpha_k=0$ (for every $k\in\{0,\cdots,n\}$) and thus, the state constraints are satisfied. We compare in Table 1 the solutions obtained for these to different types of initialization values. These results show that the algorithm is more efficient when the optimal solution of the linearized problem is chosen as an initial guess.

In Table 1, the comparison is made with V given by (4.10), the target $h^f=\mathtt{1}$ and the state constraint given by (1.3) with $c=\mathtt{0.3}$. The number of discretization points is given by $n+1$, $T^\star$ is the optimal time obtained, N_{SQP} is the number of iterations inside the SQP algorithm and T_{CPU} returns the CPU time used for computations.

In addition, the optimal solution for the nonlinear optimization problem (4.9) obtained with the initial value (4.12) does not look as good as the optimal solution obtained from the optimal solution of the linearized problem (3.6) (see in comparison Figure 2 and Figure 3).

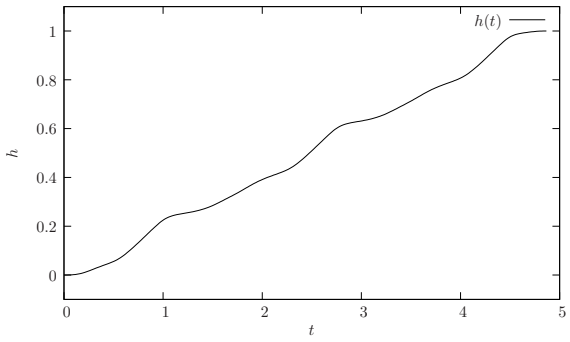

(a) displacement $t \mapsto h(t)$

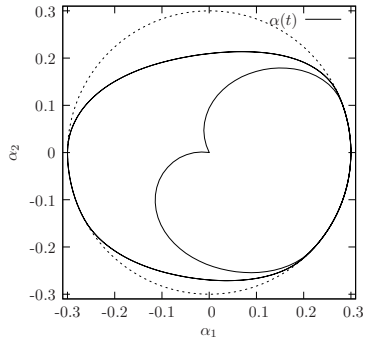

(b) trajectory of $t \mapsto \alpha(t)$

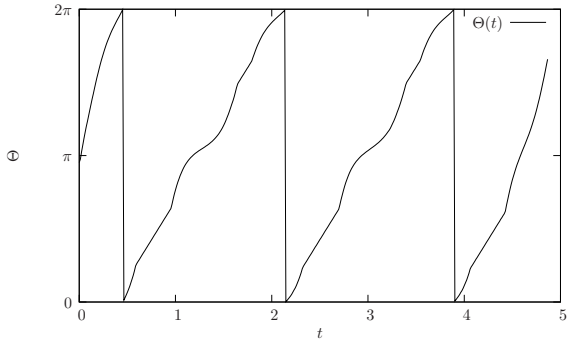

(c) solution $t \mapsto \Theta(t) \bmod 2\pi$

Figure 2: Solution of the time optimal problem (1.1)-(1.4) with V given by (4.10). The objective is $h^f = 1$, the constraint parameter c is 0.3 and the number of discretization points n is 300. Numerically, we obtain a minimal time $T = 4.866577$.

n	$T^\star$	N_{SQP}	T_{CPU} (s)
50	5.14982	716	26.532
100	4.87109	1340	102.685
150	5.31835	3861	764.928
200	4.96607	1425	291.104
250	5.17521	242	63.278
300	5.12574	1096	546.292
350	4.87108	685	363.426
400	Not converging		
450	5.00869	287	287.430
500	5.07592	364	580.006

(a) Initialisation with the initial value (4.12)

n	$T^\star$	N_{SQP}	T_{CPU} (s)
50	4.87770	79	3.380
100	4.86974	108	7.381
150	4.86779	135	18.636
200	4.86710	191	32.064
250	4.86676	200	41.511
300	4.86658	213	64.223
350	4.86646	270	123.074
400	4.86721	143	102.644
450	4.86661	157	155.655
500	4.86636	206	389.241

(b) Initialisation with the optimal control obtained for the linearized problem (3.6)

Table 1: Comparison of the results for the two different types of initialisations with the SQP algorithm.

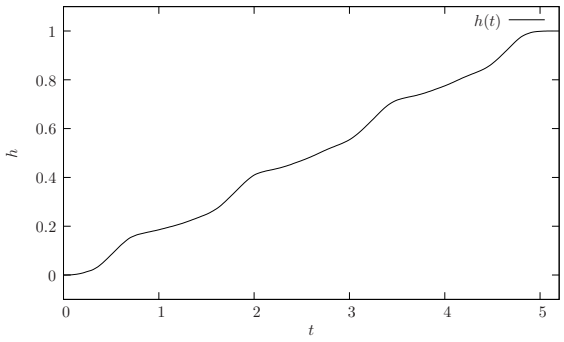

(a) displacement $t \mapsto h(t)$

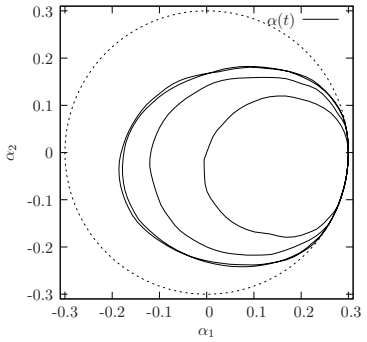

(b) trajectory of $t \mapsto \alpha(t)$

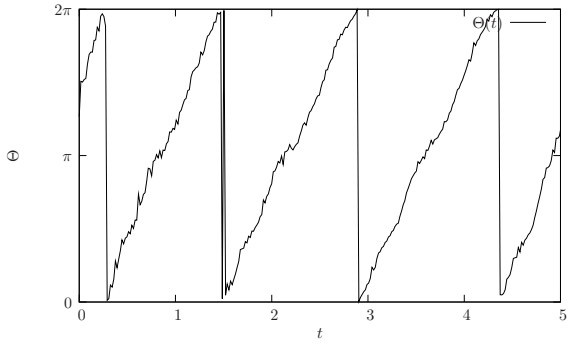

(c) solution $t \mapsto \Theta(t) \bmod 2\pi$

Figure 3: Solution of the time optimal problem (1.1)-(1.4) with V given by (4.10). The objective is $h^f = 1$, the constraint parameter c is `0.3` and the number of discretization points n is `300`. The SQP algorithm has been initialized with the initial value (4.12).

5 Application to time optimal micro-swimmers

Understanding the motion of micro-organisms is a challenging issue since at their size the fluid forces are only viscous forces and micro-organisms live in a world where inertia does not exist. Despite the pioneer works modeling and analysing the motions of micro-swimmers (see for instance [29, 19, 18, 25, 11, 28, 27]), the swimming of micro-organisms has only been recently tackled as a control problem. A lot of controllability results for various swimmers has been obtained (see for instance [4, 5, 24, 26, 23] for axi-symmetric swimmers, [3, 21] for general swimmers or [6, 12] when the fluid domain is not the whole space $\mathbb{R}^3$).

Let us also point out that numerical strategy for axi-symmetric swimmers have already been presented in [2]. The work explained in this note can be seen as an improvement of this numerical strategy when the cost function is reduced to the final time.

In this section, we consider a micro-swimmer performing axi-symmetric deformations. We denote by $(\mathbf{e}_1, \mathbf{e}_2, \mathbf{e}_3)$ the canonical basis of $\mathbb{R}^3$ and we assume that $\mathbf{e}_1$ represents the symmetry axis. At any time, the swimmer will be diffeomorphic to the unit sphere of $\mathbb{R}^3$ and its shape at rest is the unit sphere S_0.

The control problem is the following: starting from the initial location 0, reach the final position $h^f \mathbf{e}_1$ by shape changes such that at the initial and final positions, the swimmer is the unit sphere of $\mathbb{R}^3$.

For those swimmers, we will study the time optimal controllability of the dynamical system associated to the swimming problem.

5.1 Modeling and problem formulation

5.1.1 Axi-symmetric coordinates

Since we are considering axi-symmetric swimmers, we introduce the spherical coordinate system $(r, \theta, \phi) \in \mathbb{R}_+ \times [0, \pi] \times [0, 2\pi)$. For every $x = (x_1 \ x_2 \ x_3)^\top \in \mathbb{R}^3$, the spherical coordinates $(r, \theta, \phi) = \big(r(x), \theta(x), \phi(x)\big)$ are such that:

$$x = r \begin{pmatrix} \cos\theta \\ \sin\theta\cos\phi \\ \sin\theta\sin\phi \end{pmatrix} \qquad (x \in \mathbb{R}^3\,, (r, \theta, \phi) \in \mathbb{R}_+ \times [0, \pi] \times [0, 2\pi))\,,$$

with the associated local system of unit vectors $(\mathbf{e}_r, \mathbf{e}_\theta, \mathbf{e}_\phi)$ given by (see Figure 4):

$$\mathbf{e}_r = \begin{pmatrix} \cos\theta \\ \sin\theta\cos\phi \\ \sin\theta\sin\phi \end{pmatrix}, \qquad \mathbf{e}_\theta = \begin{pmatrix} -\sin\theta \\ \cos\theta\cos\phi \\ \cos\theta\sin\phi \end{pmatrix} \quad \text{and} \quad \mathbf{e}_\phi = \begin{pmatrix} \cos\theta \\ -\sin\theta\sin\phi \\ \sin\theta\cos\phi \end{pmatrix}.$$

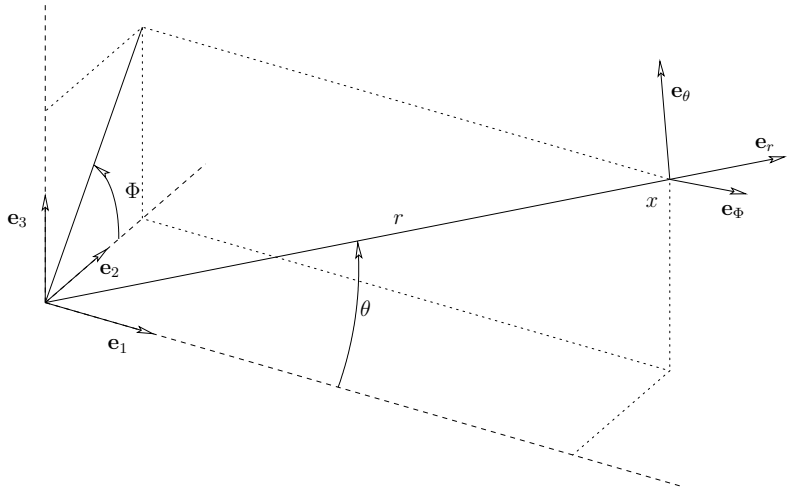

Figure 4: Spherical coordinates.

5.1.2 Swimmer's deformations

The shape of the swimmer at rest is the unit ball of $\mathbb{R}^3$ which forms the reference shape denoted by S_0. We assume that the deformation of the swimmer is axi-symmetric with respect to the symmetry axis $\mathbf{e}_1$. More precisely, we assume that the deformation X is built from two elementary deformations D_1 and D_2, that is

$$X(t, x) = x + \alpha_1(t) D_1(x) + \alpha_2(t) D_2(x)\,, \qquad (t \geqslant 0\,,\ x \in \mathbb{R}^3)\,, \tag{5.13}$$

where D_1 and D_2 are axi-symmetric and radial deformations, i.e.

$$D_i(x) = r(x)\delta_i(\theta(x))\mathbf{e}_r(x) \qquad (t \geqslant 0\,,\ x \in \mathbb{R}^3\,,\ i \in \{1, 2\})\,, \tag{5.14}$$

with $\delta_i \in C^1([0, \pi], \mathbb{R})$ and $\alpha_i \in L^\infty(\mathbb{R}_+, \mathbb{R})$ such that:

$$\alpha_1(t)\delta_1(\theta) + \alpha_2(t)\delta_2(\theta) > -1 \qquad (t \geqslant 0\,,\ \theta \in [0, \pi])\,, \tag{5.15}$$

so that $X(t,\cdot)$ is a C^1-diffeomorphism on S_0. In practice, we will consider $c>0$ small enough such that (1.3) implies (5.15). We define the domain $\mathcal{S}(t)$ occupied by the deformed swimmer at time t in the reference frame attached to the swimmer:

$$\mathcal{S}(t) = X(t, S_0) \subset \mathbb{R}^3 \qquad (t \geqslant 0)\,.$$

We also assume that the deformation X does not produce any translation. To this end, we introduce the mass density $\rho_0(x) = 1$ in the shape of the swimmer S_0 at rest and we assume that the mass is locally preserved during the deformation, that is to say that the density of the swimmer at any time $t \geqslant 0$ is given by:

$$\rho(t, X(t,x)) = \frac{1}{|\mathrm{Jac}X(t,x)|} \qquad (t \geqslant 0\,,\ x \in S_0)\,,$$

where $\mathrm{Jac}X(t,\cdot)$ denotes the Jacobian of the mapping $X(t,\cdot)$. According to (5.13) and (5.14) we have:

$$\rho(t, X(t,x)) = \frac{1}{(1+\alpha_1(t)\delta_1(\theta(x)) + \alpha_2(t)\delta_2(\theta(x)))^3} \qquad (t \geqslant 0\,,\ x \in S_0)\,.$$

With this mass density, we have, for all $t \geqslant 0$:

$$\int_{\mathcal{S}(t)} \rho(t,x)\,\mathrm{d}x = \int_{S_0} \mathrm{d}x := m_0 \tag{5.16}$$

and the mass center of the swimmer is given by:

$$\begin{aligned}
\int_{\mathcal{S}(t)} x\rho(t,x)\,\mathrm{d}x &= \int_{S_0} (x + \alpha_1(t)D_1(x) + \alpha_2(t)D_2(x))\,\mathrm{d}x \\
&= \int_0^\pi \int_0^1 \int_0^{2\pi} r\,(1 + \alpha_1(t)\delta_1(\theta) + \alpha_2(t)\delta_2(\theta))\,\mathbf{e}_r(\theta,\phi)\,r^2\sin\theta \mathrm{d}\phi\mathrm{d}r\mathrm{d}\theta \\
&= \left(\alpha_1(t)\frac{\pi}{2}\int_0^\pi \delta_1(\theta)\cos\theta\sin\theta\,\mathrm{d}\theta + \alpha_2(t)\frac{\pi}{2}\int_0^\pi \delta_2(\theta)\cos\theta\sin\theta\,\mathrm{d}\theta\right)\mathbf{e}_1\,,
\end{aligned}$$

Consequently, we assume:

$$\int_0^\pi \delta_i(\theta)\sin(2\theta)\,\mathrm{d}\theta = 0 \qquad (i \in \{1,2\})\,, \tag{5.17}$$

so that the mass center of the swimmer does not move with the deformation X.

Finally, let us consider the domain $\mathcal{S}^\dagger(t)$ occupied by the swimmer in the fluid at time $t \geqslant 0$, which is given by

$$\mathcal{S}^\dagger(t) = \mathcal{S}(t) + h(t)\mathbf{e}_1. \tag{5.18}$$

Since we have assumed that the deformation X does not introduce any translation, $h(t)\mathbf{e}_1$ is the mass center position of the swimmer in the fluid domain at time t. The domains S_0, $\mathcal{S}(t)$ and $\mathcal{S}^\dagger(t)$ are depicted on Figure 5.
In terms of the control theory, $\alpha = (\alpha_1,\ \alpha_2)^\top$ is the system's input and h is its output we aim to control.

5.1.3 Micro-swimmer and fluid flow

It is well known that the system governing the motion of a micro-swimmer is inertia less (see for instance [20, § 5.3] or [11]) and reduced to the following problem coupling,

- the Stokes equation:

$$-\Delta \boldsymbol{u} + \nabla p = 0 \qquad \text{in } \mathcal{F}(t)\,, \tag{5.19a}$$

$$\mathrm{div}\,\boldsymbol{u} = 0 \qquad \text{in } \mathcal{F}(t)\,, \tag{5.19b}$$

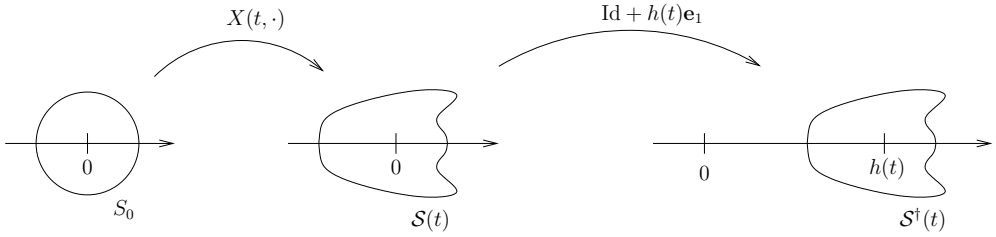

Figure 5: The deformation X and the translation $h\mathbf{e}_1$ of the swimmer.

where $\mathcal{F}(t) = \mathbb{R}^3 \setminus \mathcal{S}(t)$ and with

$$\lim_{|x|\to\infty} \boldsymbol{u}(t,x) = 0\,; \tag{5.19c}$$

- the boundary condition (continuity of the velocity at the boundary of the micro-swimmer):

$$\boldsymbol{u}(t,x) = \dot{h}(t)\mathbf{e}_1 + \big(\dot{\alpha}_1(t) D_1\left(X(t,\cdot)^{-1}(x)\right) + \dot{\alpha}_2(t) D_2\left(X(t,\cdot)^{-1}(x)\right)\big)\,\mathbf{e}_r\left(X(t,\cdot)^{-1}(x)\right)\,; \tag{5.20}$$

- quasi-static Newton law:

$$0 = \mathbf{F}(t)\cdot\mathbf{e}_1\,, \tag{5.21}$$

where $\mathbf{F}(t) = \displaystyle\int_{\partial\mathcal{S}(t)} \sigma(\boldsymbol{u},p)\mathbf{n}\,\mathrm{d}\Gamma$ with $\sigma(\boldsymbol{u},p) = \big(\nabla\boldsymbol{u} + (\nabla\boldsymbol{u})^\top\big) - p\mathrm{I}_3$ is the Cauchy stress tensor.

The well posedness of (5.19) follows from [14], where the limit (5.19c) has to be understood in a weak sense (that is $\sqrt{1+|x|^2}\boldsymbol{u}(x) \in L^2(\mathcal{F})^3$). More precisely, we have $(\boldsymbol{u},p) \in W^1_0(\mathcal{F}(t))^3 \times L^2(\mathcal{F}(t))$ where we have set:

$$W^1_0(\mathcal{F}(t)) = \left\{\varphi \in L^2_{loc}(\mathcal{F}(t))\,,\ \nabla\varphi \in L^2(\mathcal{F}(t))^3\,,\ \sqrt{1+|x|^2}\varphi \in L^2(\mathcal{F}(t))\right\}.$$

This ensures that $\boldsymbol{u}|_{\partial\mathcal{F}(t)} \in H^{\frac12}(\partial\mathcal{F}(t))$ and consequently, the expression $\displaystyle\int_{\partial\mathcal{S}(t)} \sigma(\boldsymbol{u},p)\mathbf{n}\,\mathrm{d}\Gamma$ is seen as a duality product (since $\sigma(\boldsymbol{u},p)\mathbf{n} \in H^{\frac{-1}{2}}(\partial\mathcal{S}(t))^3$ and $1 \in H^{\frac12}(\partial\mathcal{S}(t))$).

5.1.4 A geometric control problem

Let us first notice that in the full system (5.19)–(5.21) the time does not appear directly but only through the parameter $\alpha(t)$. Consequently, we define $\mathcal{S}(\alpha)$ as the image of S_0 by the map $X(\alpha) : x \in \mathbb{R}^3 \mapsto x + \alpha_1 D_1(x) + \alpha_2 D_2(x) \in \mathbb{R}^3$, for $\alpha \in \mathbb{R}^2$ such that (5.15) holds. For convenience, we also define the corresponding fluid domain $\mathcal{F}(\alpha) = \mathbb{R}^3 \setminus \mathcal{S}(\alpha)$.

For every $\alpha \in \mathbb{R}^2$ satisfying (5.15), we define $(\boldsymbol{u}_0^\alpha, p_0^\alpha)$ the solution of:

$$-\Delta\boldsymbol{u}_0^\alpha + \nabla p_0^\alpha = 0 \qquad \text{in } \mathcal{F}(\alpha)\,, \tag{5.22a}$$
$$\operatorname{div}\boldsymbol{u}_0^\alpha = 0 \qquad \text{in } \mathcal{F}(\alpha)\,, \tag{5.22b}$$
$$\lim_{|x|\to\infty} \boldsymbol{u}_0^\alpha(x) = 0\,, \tag{5.22c}$$
$$\boldsymbol{u}_0^\alpha(x) = \mathbf{e}_1, \quad \text{for all } x \in \partial\mathcal{S}(\alpha) \tag{5.22d}$$

and for $i \in \{1,2\}$, $(\boldsymbol{u}_i^\alpha, p_i^\alpha)$ is the solution of:

$$-\Delta\boldsymbol{u}_i^\alpha + \nabla p_i^\alpha = 0 \qquad \text{in } \mathcal{F}(\alpha)\,, \tag{5.23a}$$
$$\operatorname{div}\boldsymbol{u}_i^\alpha = 0 \qquad \text{in } \mathcal{F}(\alpha)\,, \tag{5.23b}$$

$$\lim_{|x|\to\infty} \boldsymbol{u}_i^\alpha(x) = 0\,, \tag{5.23c}$$

$$\boldsymbol{u}_i^\alpha(x) = D_i\left(X(\alpha)^{-1}(x)\right), \quad \text{for all } x \in \partial\mathcal{S}(\alpha) \tag{5.23d}$$

Then, by decomposing the solution $(\boldsymbol{u}(t,\cdot), p(t,\cdot))$ of (5.19)-(5.20) in terms of $\{(u_i^\alpha, p_i^\alpha)\}_{i\in\{0,1,2\}}$ and due to the linearity of the Cauchy stress tensor, relation (5.21) becomes:

$$\dot{h}(t)\mathbf{F}_0(\alpha(t))\cdot\mathbf{e}_1 = -\left(\dot{\alpha}_1(t)\mathbf{F}_1(\alpha(t)) + \dot{\alpha}_2(t)\mathbf{F}_2(\alpha(t))\right)\cdot\mathbf{e}_1\,, \tag{5.24}$$

where for every $i \in \{0,1,2\}$ and every $\alpha \in \mathbb{R}^2$ satisfying (5.15), we have set:

$$\mathbf{F}_i(\alpha) = \int_{\partial\mathcal{S}(\alpha)} \sigma(\boldsymbol{u}_i^\alpha, p_i^\alpha)\mathbf{n}\,\mathrm{d}\Gamma \tag{5.25}$$

with $\sigma(\boldsymbol{u}_i^\alpha, p_i^\alpha) = \left(\nabla\boldsymbol{u}_i^\alpha + (\nabla\boldsymbol{u}_i^\alpha)^\top\right) - p_i^\alpha \mathrm{I}_3$.

By Green formula, we have:

$$\mathbf{e}_1 \cdot \int_{\partial\mathcal{F}} \sigma(\boldsymbol{u}_0, p_0)\mathbf{n}\,\mathrm{d}\Gamma = 2\int_{\mathcal{F}} \mathrm{D}(\boldsymbol{u}_0) : \mathrm{D}(\boldsymbol{u}_0)\,\mathrm{d}x > 0\,.$$

Consequently, $\mathbf{F}_0(\alpha)\cdot\mathbf{e}_1 \neq 0$ and the control problem can be recast as the generalized Brockett system (1.1) with

$$V(\alpha) = \frac{-1}{\mathbf{F}_0(\alpha)\cdot\mathbf{e}_1}\begin{pmatrix}\mathbf{F}_1(\alpha)\cdot\mathbf{e}_1\\ \mathbf{F}_2(\alpha)\cdot\mathbf{e}_1\end{pmatrix}. \tag{5.26}$$

This system form has been already establish in the pioneer work of F. Alouges, A. DeSimone and A. Lefebvre [5].
Notice that even if α represents the physical control of the swimming system, it is more convenience for analysis to consider $\lambda = \dot{\alpha}$ as the control variable. This will also allow us to control both the shape and the position of the swimmer.

We also set the initial conditions (1.1c) for this system and the target position to be reached in a time $T > 0$ is given by (1.2). These initial and final conditions mean that the micro-swimmer is the unit sphere located at the origin at initial time and a unit sphere located in $h^f\mathbf{e}_1$ at final time T.

We point out that a state constraint on α is needed to be able to well define $\mathbf{F}_i(\alpha(t))$ for every time $t \geqslant 0$. This constraint is given by (5.15).

In addition, according to [21, Lemma 1] or [23, Theorem 2.6], there exists $c > 0$ small enough, such that the mapping $\alpha \in \mathbb{R}^2 \mapsto V(\alpha) \in \mathbb{R}^2$ with V defined by (5.26) is of regularity C^∞ on $B_0(2c)$. Consequently, we chose $c > 0$ small enough such that this condition holds together with (5.15).

Remark 5.1. *From [23], there exists δ_1, $\delta_2 \in C^1([0,\pi],\mathbb{R})$ in* (5.15) *such that $\nabla V(0)$ is not symmetric. Moreover, using the arguments of [21], this situation is generic.*

5.2 Numerical computation of a time optimal trajectory

Let us consider the deformations D_1 and D_2 similar to the one given in [23], that is to say that D_1 and D_2 are given by (5.14) with

$$\delta_1(\theta) = P_2(\cos\theta) \qquad \text{and} \qquad \delta_2(\theta) = P_3(\cos\theta)\,, \tag{5.27}$$

where P_2 (resp. P_3) is the Legendre polynomial of order 2 (resp. 3). With these two elementary deformations, we obtain from [27],

$$V(0) = 0 \qquad \text{and} \qquad \nabla V(0) = \begin{pmatrix} 0 & \frac{6}{35}\\ \frac{4}{15} & 0\end{pmatrix}.$$

These expressions allow us to compute the explicit form of the time optimal controls for the approximate linearized system (3.6).

In order to numerically compute the fluid forces $\mathbf{F}_i(\alpha)\cdot\mathbf{e}_1$ for $i\in\{0,1,2\}$, we use the spherical harmonics expansion of the exterior Stokes solution given in [8] (see also [15] or [27]). Then, we compute the time optimal controls by using the direct discretization method explained in section 4. The initial guess for the discrete nonlinear optimization problem is chosen as the explicit optimal solution of the approximate linear control problem (3.6) given in Proposition 3.1. We expect that the approximate optimal deformation for the linearized problem is close to the optimal solution for the nonlinear problem, so that the direct method will converge quickly.

We apply this computational method with the deformation D_1 and D_2 given above through Legendre polynomials and we choose $c=0.3$ and $h^f=\frac{1}{2}$. The optimal trajectories for h and α are depicted on Figure 6. The optimal time is $T^\star\simeq 48.9$.

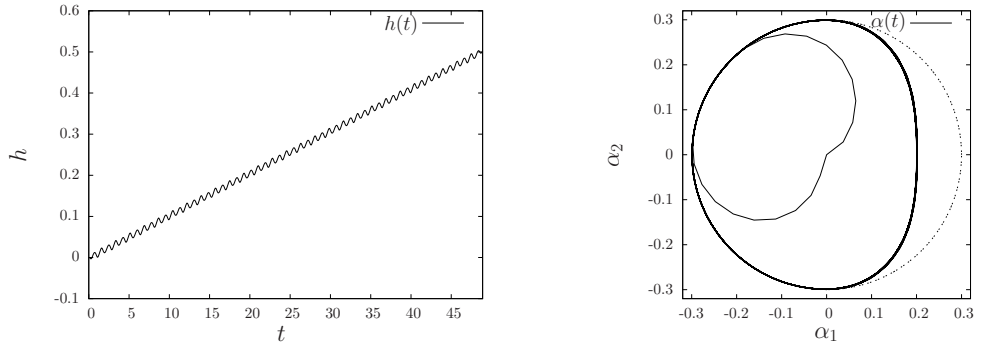

(a) Optimal trajectory for h. (b) Optimal trajectory for α.

Figure 6: Optimal trajectories for the system (1.1), (1.2)–(1.4) with V given by (5.26) together with the deformations D_1 and D_2 defined by (5.14) with (5.27). In addition, we have set $c=0.3$ and $h^f=\frac{1}{2}$.

We numerically observe on Figure 6 that the optimal trajectory for α is mainly periodic. On Figure 7, we also give the optimal trajectory of h during a period in time and finally we plot on Figure 8 the different shapes of the swimmer under the optimal deformation for different instants in the time period .

6 Conclusion

In this note, we have presented a numerical strategy for solving a time minimal control problem for a nonlinear system which generalizes the Brockett integrator. This method is based on the explicit computation of time optimal controls for a state constraint Brockett system which approximates the original nonlinear control problem. These explicit solutions are used as initial guesses in the nonlinear problem. Numerical tests have shown the good behavior of this strategy. This numerical method is then applied to a time optimal control problem for micro-swimmer with shape changes. The shapes of the swimmer are small deformations of the unit sphere. Despite two elementary deformations are used for the swimmer's shapes, it is easy to extend this work to the case of a finite number of elementary deformations.

Finally, we observe numerically that the optimal trajectory for α is mainly periodic. It would be interesting to prove rigorously this property. For instance, one could expect the following result : for $|h^f|$ large enough and for $\alpha\in A$ with A a compact set of $\mathbb{R}^2$, the trajectory of α is composed by one starting curve followed by a periodic curve and ending with a final curve. Such a result would be a real improvement for numerical computations since we would only have to solve three simpler (but coupled) time optimal control problems.

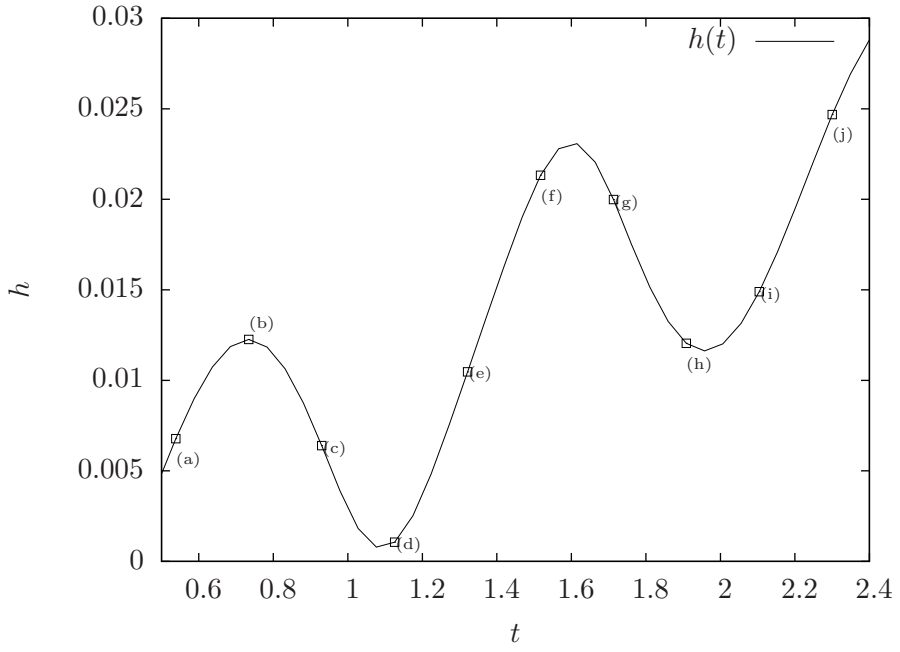

Figure 7: Optimal trajectory of h between $t_0 = 0.5384$ and $t_1 = 2.3002$ corresponding to one period of α.

References

[1] A. A. Agrachev and Y. L. Sachkov. *Control theory from the geometric viewpoint*, volume 87 of *Encyclopaedia of Mathematical Sciences*. Springer-Verlag, Berlin, 2004. Control Theory and Optimization, II.

[2] F. Alouges, A. Desimone, and L. Heltai. Numerical strategies for stroke optimization of axisymmetric microswimmers. *Math. Models Methods Appl. Sci.*, 21(2):361–387, 2011.

[3] F. Alouges, A. DeSimone, L. Heltai, A. Lefebvre-Lepot, and B. Merlet. Optimally swimming Stokesian robots. *Discrete Contin. Dyn. Syst., Ser. B*, 18(5):1189–1215, 2013.

[4] F. Alouges, A. Desimone, and A. Lefebvre. Optimal strokes for low Reynolds number swimmers: An example. *J. Nonlinear Sci.*, 18(3):277–302, 2008.

[5] F. Alouges, A. DeSimone, and A. Lefebvre. Optimal strokes for axisymmetric microswimmers. *The European Physical Journal E*, 28(3):279–284, 2009.

[6] F. Alouges and L. Giraldi. Enhanced controllability of low Reynolds number swimmers in the presence of a wall. *Acta Appl. Math.*, 128(1):153–179, 2013.

[7] J. F. Bonnans, J. C. Gilbert, C. Lemaréchal, and C. A. Sagastizábal. *Numerical optimization*. Universitext. Springer-Verlag, Berlin, second edition, 2006. Theoretical and practical aspects.

[8] H. Brenner. The stokes resistance of a slightly deformed sphere. *Chemical Engineering Science*, 19(8):519 – 539, 1964.

[9] R. H. Byrd, M. E. Hribar, and J. Nocedal. An interior point algorithm for large-scale nonlinear programming. *SIAM J. Optim.*, 9(4):877–900, 1999. Dedicated to John E. Dennis, Jr., on his 60th birthday.

[10] L. Cesari. *Optimization—theory and applications*, volume 17 of *Applications of Mathematics (New York)*. Springer-Verlag, New York, 1983. Problems with ordinary differential equations.

[11] S. Childress. *Mechanics of swimming and flying*, volume 2 of *Cambridge Studies in Mathematical Biology*. Cambridge University Press, Cambridge, 1981.

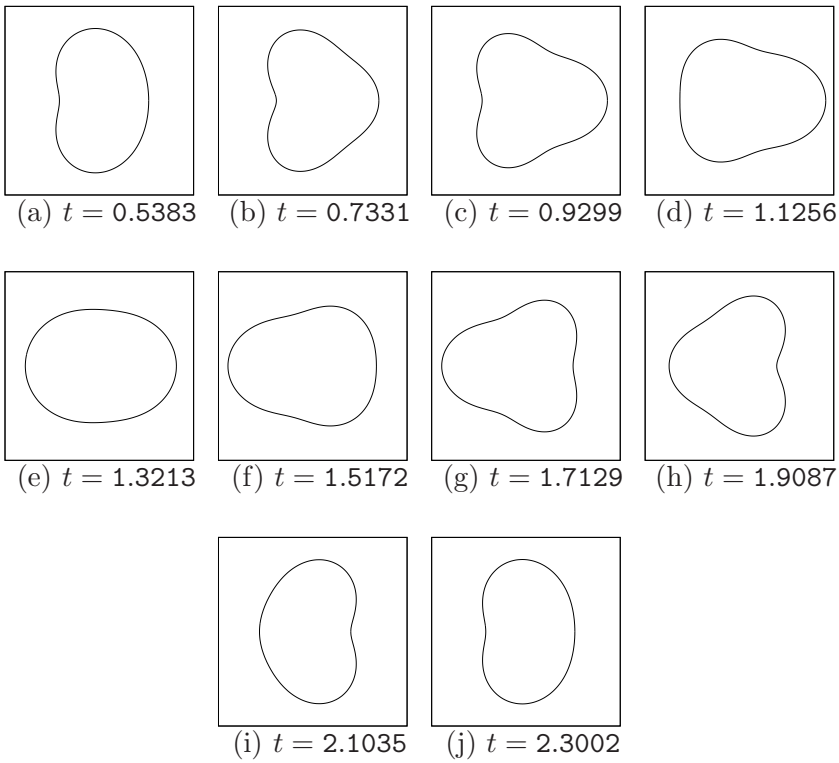

Figure 8: Optimal shapes of the swimmer between $t_0 = 0.5384$ and $t_1 = 2.3002$.

[12] D. Gérard-Varet and L. Giraldi. Rough wall effect on micro-swimmers. Sept. 2013.

[13] P. E. Gill, W. Murray, and M. H. Wright. *Practical optimization*. Academic Press, Inc., London-New York, 1981.

[14] V. Girault and A. Sequeira. A well-posed problem for the exterior Stokes equations in two and three dimensions. *Arch. Rational Mech. Anal.*, 114(4):313–333, 1991.

[15] J. Happel and H. Brenner. *Low Reynolds number hydrodynamics with special applications to particulate media*. Prentice-Hall Inc., Englewood Cliffs, N.J., 1965.

[16] R. F. Hartl, S. P. Sethi, and R. G. Vickson. A survey of the maximum principles for optimal control problems with state constraints. *SIAM Rev.*, 37(2):181–218, 1995.

[17] V. Jurdjevic. *Geometric control theory*, volume 52 of *Cambridge Studies in Advanced Mathematics*. Cambridge University Press, Cambridge, 1997.

[18] J. Lighthill. *Mathematical biofluiddynamics*. Society for Industrial and Applied Mathematics, Philadelphia, Pa., 1975. Based on the lecture course delivered to the Mathematical Biofluiddynamics Research Conference of the National Science Foundation held from July 16–20, 1973, at Rensselaer Polytechnic Institute, Troy, New York, Regional Conference Series in Applied Mathematics, No. 17.

[19] M. J. Lighthill. On the squirming motion of nearly spherical deformable bodies through liquids at very small Reynolds numbers. *Comm. Pure Appl. Math.*, 5:109–118, 1952.

[20] J. Lohéac. *Time optimal control and low Reynolds number swimming*. Theses, Université de Lorraine, Dec. 2012.

[21] J. Lohéac and A. Munnier. Controllability of 3D low Reynolds number swimmers. *ESAIM, Control Optim. Calc. Var.*, 20(1):236–268, 2014.

[22] J. Lohéac and J.-F. Scheid. Time optimal control for a nonholonomic system with state constraint. *Math. Control Relat. Fields*, 3(2):185–208, 2013.

[23] J. Lohéac, J.-F. Scheid, and M. Tucsnak. Controllability and time optimal control for low reynolds numbers swimmers. *Acta Applicandae Mathematicae*, 123:175–200, 2013.

[24] S. Michelin and E. Lauga. Efficiency optimization and symmetry-breaking in a model of ciliary locomotion. *Physics of fluids*, 22:111901, 2010.

[25] E. Purcell. Life at low Reynolds number. *American Journal of Physics*, 45:3–11, June 1977.

[26] J. San Martin, T. Takahashi, and M. Tucsnak. A control theoretic approach to the swimming of microscopic organisms. *Q. Appl. Math.*, 65(3):405–424, 2007.

[27] A. Shapere and F. Wilczek. Efficiencies of self-propulsion at low Reynolds number. *J. Fluid Mech.*, 198:587–599, 1989.

[28] A. Shapere and F. Wilczek. Geometry of self-propulsion at low Reynolds number. *J. Fluid Mech.*, 198:557–585, 1989.

[29] G. Taylor. Analysis of the swimming of microscopic organisms. *Proc. Roy. Soc. London. Ser. A.*, 209:447–461, 1951.

[30] E. Trélat. *Contrôle optimal*. Mathématiques Concrètes. [Concrete Mathematics]. Vuibert, Paris, 2005. Théorie & applications. [Theory and applications].